Macromolecules **1992,** *25,* 743–749

Polyion Conformation and Second Virial Coefficient Dependences on the Ionic Strength for Flexible Polyelectrolyte Solutions

Hedi Mattoussi,* Steve O'Donohue,† and Frank E. Karasz

Polymer Science and Engineering Department, University of Massachusetts, Amherst, Massachusetts 01003

Received February 26, 1991; Revised Manuscript Received August 26, 1991

ABSTRACT: Using small-angle light-scattering technique, we measured the macromolecular size, the second virial coefficient, and the molecular weight for a polyelectrolyte material with flexible chains in dilute solutions and with moderate to high ionic strengths. The macromolecular size R_G is found to be very much dependent on the solution ionic strength. The chains continuously change their conformation from an expanded state to a more compact form, as the screening effects brought by the counterion excess become more important when the ionic strength of the medium increases. The second virial coefficient A_2 also decreases with increasing ionic strength. This set of data has been analyzed within the framework of a wormlike chain with electrostatic contributions to the persistence length ρ. This treatment was based on neglecting of the electrostatic contribution to the excluded volume parameter and on the fact that the neutral term of the latter is small. Incidentally, this set of measurements provided us with information about the molecular weight M_W, a parameter difficult to obtain with good accuracy for the present material (charged macromolecules) using techniques such as GPC.

I. Introduction

The properties of polymer solutions depend, very much, on the inherent nature of the macromolecules and the interactions between solute–solute and solute–solvent monomers.[1–5] Within the macromolecule, short-distance interactions are often characterized by the parameter persistence length ρ, which describes the local stiffness of the chain.[1,3,6,7] Conversely, the long-range interactions depend on the excluded volume parameter υ.[1–5] The second virial coefficient A_2 describes the interactions between solute and solvent molecules for dilute solutions.[1–5,8] It also accounts for interactions between solute monomers.

The chain radius of gyration R_G is expressed as[3,7–10]

$$R_G^{\ 2} = \alpha^2 \frac{L_W \rho}{3} \Psi\left[\frac{L_W}{\rho}\right] \tag{1}$$

where L_W is the contour length, $\Psi(y)$ is a dimensionless function expressed as $\Psi(y) = \{1 + 4(y^{-1})\}^{-1}$ for large L_W and $\Psi(y) \rightarrow 1$ for $L_W/\rho \gg 1$, and α is the expansion factor of the macromolecule with respect to the wormlike case. For flexible polymers, α may be defined as[3]

$$\alpha = 1 + {}^4/_3 z + ... \tag{2}$$

where z is a function of the excluded volume parameter and may expressed as[3,4]

$$z = \left[\frac{3}{2\pi a^2}\right]^{3/2} \upsilon N^{1/2} \tag{3}$$

where a is the monomer size and N is the number of monomer units in the chain. An "extensive" expression for the second virial coefficient A_2 is written, for long flexible macromolecules in good solvent, as[3,8]

$$A_2 \simeq \frac{16\pi N_A R_G^{\ 3}}{3^{3/2} M_W^{\ 2}} \ln \left\{1 + \frac{\pi^{1/2}}{2}(\alpha^2 - 1)\right\} \tag{4}$$

where N_A and M_W designate the Avogadro number and the average molecular weight of the solute macromolecules, respectively. It reduces to zero for a Gaussian chain in Θ solvent where $\alpha \simeq 1$.[8]

For polyelectrolyte solutions, the Coulomb interactions between charges, fixed along the macromolecule backbone, affect all these parameters. These interactions are also very sensitive to the presence of counterions. The addition of electrolyte(s) to the medium, which monitors the solution ionic strength, screens out the repulsive interactions between charges along the chain. The competition between repulsive forces, along the fixed charges on the chain, and the screening effects brought by the counterion excess are manifested in a progressive and complex dependence of the solution properties on these parameters (charge density and counterion excess). A parameter often used to account for the competition between the electrostatic repulsions and screening effects is the Debye–Huckel (DH) screening length κ^{-1}.[2,11] It characterizes the distance beyond which the Coulomb repulsions between two similar charges in the solution (particularly two charges along the same polyion backbone) are strongly reduced. The Debye–Huckel parameter κ is expressed (in cgs units) as[2,9,11–13]

$$\kappa^2 = \frac{8\pi N_A c_S}{1000}\left[\frac{e^2}{\epsilon k_B T}\right] \tag{5}$$

where ϵ is the dielectric constant of the medium (solvent), c_S is the counterion concentration, e is the electron unit charge, and $k_B T$ is the Boltzmann factor. In such media, the electrostatic contributions to the parameters ρ and υ (termed ρ_e and υ_e) must be considered in order to provide a meaningful description of the thermodynamical properties of the solutions[3,11–13]

$$\rho = \rho_n + \rho_e \qquad \upsilon = \upsilon_n + \upsilon_e \tag{6}$$

where the subscript n designates the neutral case. Thus, all parameters characterizing the solutions have electrostatic contributions.

The charges carried by the polyions are the result of dipole dissociation (electrolyte dissociation) along the backbone. Such dissociation is very sensitive to the environment (solvent) polarity strength, a property characterized by the dielectric constant ϵ. Therefore, all the parameters discussed above are also affected by the

---

*Present address: Department of Chemistry, Carnegie Mellon University, 4400 Fifth Ave., Pittsburgh, PA 15213.

† Present address: Polymer Laboratories, Essex Road, Church Stretton, Shropshire SY6 6AX, United Kingdom.

0024-9297/92/2225-0743$03.00/0

polarity strength of the solvent (consequently by ϵ).

In this report, we present a contribution to the understanding of polyelectrolyte solutions in the presence of counterion excess (relatively high ionic strengths). Using static light scattering at small angles (SALS), we measured the radius of gyration R_G and the second virial coefficient A_2 and followed their respective evolution as the ionic strength of the medium was monitored. We limited our study to the case with high ionic strengths and low polymer concentrations to ensure the dilute solution features, since the polyion expansion and the electrostatic interactions effects are relatively reduced.[8,14,16–18] In fact, it is known that polyelectrolyte solutions often reach the "semidilute" regime even for very small concentrations if no counterions were added to the system, as has been proved for the present system, for instance.[14] This was attributed to the large expansion of the macromolecules caused by the Coulomb repulsions between charges along the polyion backbone.[8,11–17] In addition, departure from the linear variation of the osmotic compressibility χ_T vs c may occur for polyelectrolyte solutions even with small concentrations if the ionic strength of the medium is small.[8,28] This adds extra complexity to the analysis of light scattering at zero angle as has been reported for many polyelectrolyte materials.[8,28] We had pursued a physical study on the dynamic aspects of such media using quasi-elastic light scattering (QELS) measurements.[14] This study showed that the solutions experienced different behaviors depending on whether external counterions were added to the medium or not. For the high ionic strength case, the single-chain hydrodynamic size R_H and the interactions parameter $k_D[\eta]$ (k_D is constant, of the order of 1, and $[\eta]$ is the intrinsic viscosity) were found to be strongly dependent on the ionic strength of the solutions.[14] The present set of data complete and confirm the observations reported on the diffusion coefficient. Their discussion is done within the framework of a long flexible polymer chain with electrostatic contributions to the persistence length.

We start with a brief introduction of the general concepts for SALS, followed by a description of the experimental setup, as well as the material we used. In the next section, we discuss the experimental data with comparison to previous works either on the present material or on other systems and compare them to theoretical considerations.

II. Experimental Section

II.1. General Formulation and Experimental Setup. It has been known that a nonhomogeneous medium, e.g., polymer solution, colloidal dispersion, micelle solution, etc., subject to concentration fluctuations δc scatters light.[2,5,8,19–21] The excess in the scattered intensity with respect to the pure solvent is directly related to the structure factor $S(q,c)$ and reads as

$$I(q,c) \simeq S(q,c) = \langle \delta c(q)\, \delta c^*(q) \rangle \tag{7}$$

where q is the scattering wavevector, $q = (4\pi/\lambda)n_o \sin(\theta/2)$ with λ the incident light wavelength, n_o the solvent refractive index, and θ the scattering angle. The brackets designate the time and thermodynamic average over all conformations. Experimentally, the measured parameter often identified as the Rayleigh ratio $R(\theta)$ is defined as[5,19–21,28]

$$R(\theta,c) = \frac{r^2}{I_o(1 + \cos^2\theta)}\{I(\theta,c) - I(\theta,0)\} \tag{8}$$

where $I(\theta,c)$ is the scattered intensity at an angle θ and concentration c, r is the distance between the scattering volume and the detector, and I_o is the incident intensity. $I(\theta,0)$ designates the intensity scattered by the solvent reference. The parameter $R(\theta)$ is defined to account for the polarization factor $(1 + \cos^2\theta)$ for unpolarized light.

For polymer solutions in the dilute regime, $R(\theta)$ could be written in terms of two separate factors (form factor $S(q)$ and intermolecular structure factor $\chi_T(q,c)$)[5,8a,19–21,28]

$$R(\theta,c) = R(q,c) \simeq KcM\, S(q)\, \chi_T(q,c) \tag{9}$$

where M is the molecular weight and χ_T is the osmotic compressibility, related to the virial coefficient A_2. K is an experimental factor which for light scattering is dependent on the refractive index increment $(\partial n/\partial c)$ with respect to the solvent and reads as $K = \{(2\pi n_o^2)/(N_A\lambda^4)\}(\partial n/\partial c)^2$.[5,19–21,28] The increment $(\partial n/\partial c)$ is the equivalent of the contrast factor for X-ray or neutron scattering cases.[5]

In the limit of small concentrations ($c \ll 1$) and within the Guinier regime ($qR_G < 1$), a linear expression for the inverse of the Rayleigh ratio with c and $\sin^2(\theta/2)$ (or q) emerges:[2,5,19–22]

$$\frac{Kc}{R(\theta)} \simeq \frac{1}{M_W}\left(1 + \{(4\pi/\lambda)n_o\}^2 \frac{\sin^2(\theta/2)\, R_G^{\,2}}{3} + 2A_2M_Wc + ...\right) \tag{10}$$

The radius of gyration R_G is defined as[2,3,7,21,22]

$$R_G^{\,2} = \frac{1}{2N}\sum_{ij} \langle (\mathrm{r}_{ij}^{\,2}) \rangle \tag{11}$$

where the summation is taken over all monomers i and j in the solute macromolecule and N designates the number of monomer units in the chain.

A plot of $Kc/R(\theta)$ vs $\sin^2(\theta/2) + c$ provides a set of straight lines: a Zimm plot. From the slopes at $c = 0$ and at $\theta = 0$, one can deduce the radius of gyration of an isolated macromolecule R_G and the second virial coefficient A_2, respectively.[5,7–9,19–22] The limit $\theta = c = 0$ enables one to reach an estimate of the molecular weight M_W, knowing the experimental value of K. For the present study these three parameters are the focus of the discussion.

As experimental setup, we used a small-angle light-scattering instrument provided by Otsuka Instruments (Japan). It is operated at the He–Ne wavelength, $\lambda = 632.8$ nm, with an incident intensity of 5 mW. It is equipped with a temperature-controlled clean and index-matched bath through which liquid is continuously pumped and filtered. This setup allows a scan of angles between 10° and 150° with a 10° step. Nevertheless, the lowest value, $\theta = 10°$, was found to provide high and unstable intensity. It has not been used for the present study. Calibration measurements were done using benzene.[8,28] The excess in the scattered intensity (Rayleigh ratio, $R(\theta)$) is obtained at each given angle, as the difference between the solution and the reference (eq 8)

$$R(\theta,c) = \frac{r^2}{I_o(1 + \cos^2\theta)}\{I(\theta,c,c_S) - I(\theta,0,c_S)\} \tag{12}$$

where $I(c,c_S)$ designates the intensity provided by a solution with concentration c and at given ionic strength c_S (it is practically the salt concentration in the medium). The intensity reference $I(c_S)$ is provided by the pure solvent to which we added an amount of electrolyte to reach the ionic strength c_S.

The refractive index increments were measured at $\lambda = 632.8$ nm using a differential refractomer, Photal RM 1002 (Polymer Laboratories). The increments Δn vs c fit straight lines for each given ionic strength c_S (Figure 1). The same solutions were used for both measurements (Δn and $R(\theta)$). All curves have zero intercept at the origin, except for the highest value of c_S where a slightly positive intercept was measured. This set of solutions gave a nice Zimm plot, however. Table I provides the corresponding values for $\partial n/\partial c$ for the different c_S. The resulting value, afterward used in the data analysis, is $\partial n/\partial c = 0.25$ cm^3/g.

II.2. Materials and Sample Preparation. We used the compound poly(xylylene tetrahydrothiophenium chloride) known as the precursor of the poly(p-phenylenevinylene) (PPV).[14,23–27] The final PPV is obtained from casting of water solution of PPV precursor and heating the resulting film at high temperature, $T \simeq 300$ °C, for 2–3 h. This allows elimination of the sulfonium salt side groups. PPV is not soluble in any common known solvent. Consequently, many studies done to identify this material are pursued in solutions of the precursor. PPV has promising conducting and nonlinear optical properties, as well as interesting crystalline behavior. It has been the center of intensive interest and investigations.[14,23–27] The precursor has been synthesized by L. Frank (Lark Enterprise, MA). It was

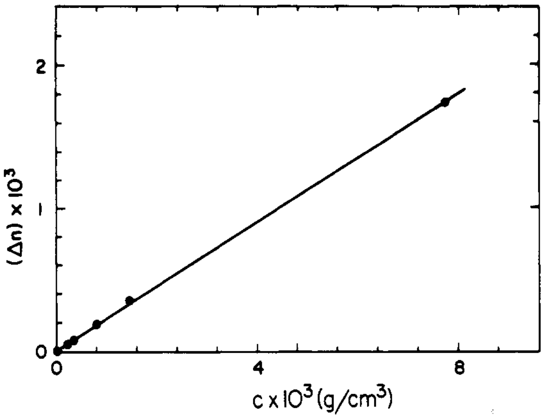

Figure 1. Experimental data of the refractive index increment Δn vs polymer concentration c at a given ionic strength, $c_S = 0.78 \times 10^{-2}$ M.

Table I
Values for the Refractive Index Increment ($\partial n/\partial c$) Together with the Corresponding Salt Concentrations Scanned

$10^2 c_S$ (M)	0.44	0.56	0.78	1.1	4.1
$\partial n/\partial c$ (cm³/g)	0.250	0.236	0.250	0.250	0.250

polymerized by anionic polymerization in water solutions starting from monomer molecules at low concentrations. Solutions with concentration of about 5% (weight) in water were provided to us. The material is, afterward, precipitated in acetone and thoroughly washed with clean water to eliminate the excess of monomer ions.[14,25,26] The resulting material is dry-pumped under a nitrogen atmosphere for several hours. This ensures the elimination of residual ions and water molecules. The resulting material is then stored in a frozen atmosphere.

To make the present solutions, we used HPLC methanol (Fisher Scientific). For each set of solutions, the solvent at a given ionic strength was first made and then used for solution preparation. The solutions are stored at low temperature and taken out for experimental use. This avoids the elimination of side sulfonium salt, slightly enhanced at higher temperatures. Each solution is filtered into the light-scattering sample using a Teflon filter (0.22-μm pore size, Millipore).[14] One or two filtrations were found sufficient to provide a clean sample for light-scattering purposes.

Early GPC measurements on a rather modified PPV precursor compound (tetrafluoroborate side groups instead of sulfonium salt), dissolved in DMF, provided an estimate for the molecular weight:[26]

$$M_W \simeq 10^6 \qquad M_W/M_n \simeq 2 \tag{13}$$

These values are not extremely accurate though, since GPC applied to polyelectrolyte solutions is often associated with difficulties.[26]

For our electrolyte, we used sodium chloride (NaCl) from Fisher. All measurements were done at a given constant temperature (room temperature, $T \simeq 25$ °C). The ionic strength of the solution is actually given by the amount of free counterions present in the medium. However, the contribution from the solute macromolecules is very small for the values of c_S used in the present study.[14] Therefore, the value for the ionic strength of the medium is taken to be the salt concentration c_S externally added, as was done in previous studies.[14]

III. Results and Discussion

Typical Zimm plots for sets of solutions at given ionic strengths are shown in Figure 2. The cases a and b correspond to two different values of salt concentrations: $c_S = 0.78 \times 10^{-2}$ M and $c_S = 4.1 \times 10^{-2}$ M (M designates moles per liter), respectively. For both cases, the inverse of the excess in the scattered intensity (Rayleigh ratio, $\{Kc/R(\theta)\}$) is linearly dependent on both $\sin^2(\theta/2)$ and c, as was predicted for dilute polymer solutions within the Guinier regime (eq 10).[2,5,19-22] However, a slight departure from the linear behavior of $\{Kc/R(\theta)\}$ vs $\sin^2(\theta/2)$ at a given c and c_S could be detected for high polymer concentrations, e.g., upper line in Figure 2a. A departure from the linear dependence of $\{Kc/R(\theta)\}$ on the polymer concentration ($\{Kc/R(\theta)\}$ vs c) becomes even more pronounced for small ionic strengths and if a plot at zero scattering angle, $\{Kc/R(\theta=0)\}$ vs c, is used (Debye plot), as shown in Figure 3 (see below). The experimental values for the radius of gyration R_G, the second virial coefficient A_2, and the molecular weight M_W hereby measured using the Zimm analysis and limited to the very dilute regime are reported in Table II, together with the corresponding salt concentrations. The use of Zimm analysis did not provide one constant value for the molecular weight. Slightly increasing values are reached for decreasing ionic strength. Also the value reached for M_W at a given ionic strength is larger if a substantially wider interval of polymer concentrations is used for the Zimm plot.[5]

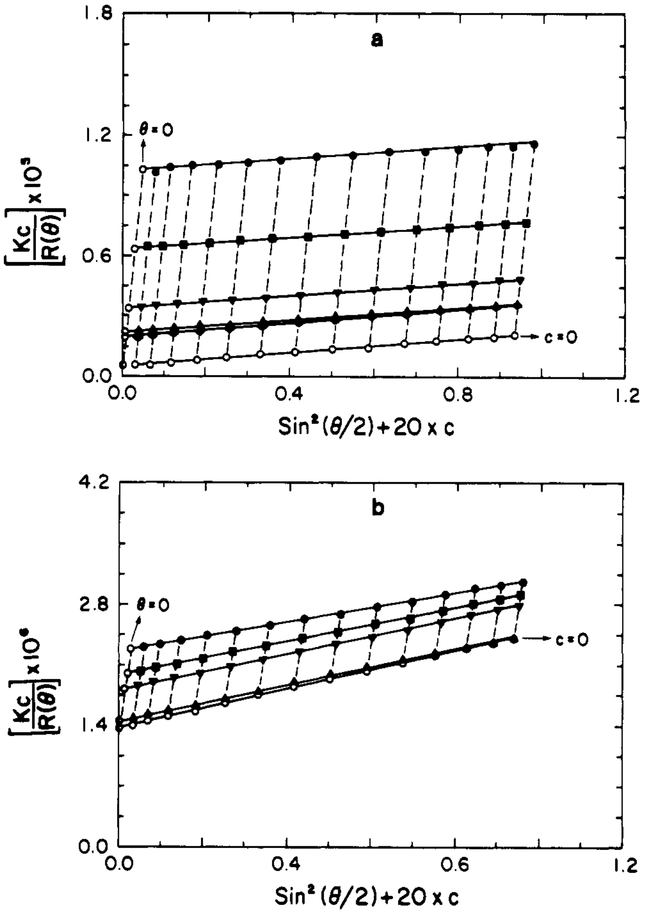

Figure 2. Two Zimm plots for the present set of solutions at different ionic strengths: (a) $c_S = 0.78 \times 10^{-2}$ M, the largest value of c shown on this plot, corresponding to $c \simeq 2.3 \times 10^{-3}$ (g/cm³), was not used in the data analysis; the latter was limited to the interval $0 < c < 1.48 \times 10^{-3}$ (g/cm³); (b) $c_S = 4.1 \times 10^{-2}$ M and polymer concentration $0 < c < 1.3 \times 10^{-3}$ (g/cm³).

However, the use of Debye analysis (a plot of $\{Kc/R(\theta=0)\}$ vs c) has provided a more accurate estimation for the molecular weight M_W: $\{Kc/R(\theta=0)\} \rightarrow 1/M_W$ for $c \rightarrow 0$. A fit of $\{Kc/R(\theta=0)\}$ vs c to an expansion involving the third virial coefficient A_3 (higher order in c) provided better agreement with the experimental data (Figure 3). The limit at $c = 0$ reached for all ionic strengths is constant within experimental uncertainties (about 10%; see Table II). It is the same limit as the one provided by Zimm analysis at $\theta = c = 0$ for the highest ionic strength ($c_S = 4.1 \times 10^{-2}$ M), where a linear expansion for the $\{Kc/R(\theta=0)\}$ vs c describes well the experimental data. This agreement is quite comforting since the final measured molecular

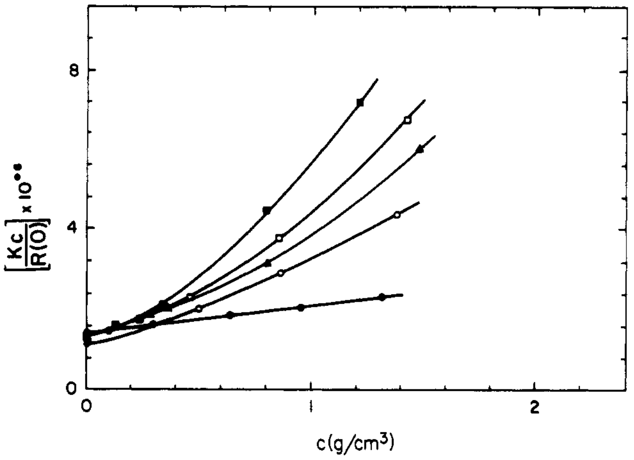

Figure 3. Plot of $\{Kc/R(\theta=0)\}$ vs polymer concentration c (Debye plot) for the different salt concentrations scanned. A fixed common extrapolated value is reached at infinite dilutions c = 0 (g/cm³): (■) $c_S \simeq 0.446 \times 10^{-2}$ M; (□) $c_S \simeq 0.56 \times 10^{-2}$ M; (▲) $c_S \simeq 0.78 \times 10^{-2}$ M; (○) $c_S \simeq 1.1 \times 10^{-2}$ M; (●) $c_S \simeq 4.1 \times 10^{-2}$ M. Nevertheless, a slight problem is associated with the case $c_S \simeq 0.56 \times 10^{-2}$ M where $\partial n/\partial c$ was slightly small (see text).

Table II
Expeimental Values for the Radius of Gyration R_G, the Second Virial Coefficient A_2, and the Molecular Weight M_W for the Ionic Strengths Studied

$10^2 c_S$ (M)	0.44	0.56	0.78	1.1	4.1
$10^{-2}(c_S)^{-1}$ (M^{-1})	2.27	1.785	1.28	0.91	0.244
$(c_S)^{-1/2}$ (M$^{-1/2}$)	14.97	13.36	11.32	9.53	4.94
		(a) Zimm Analysis			
$10^{-6}M_W$	1.45	1.39	1.27	1.27	0.75
R_G (Å)	1300	1100	992	847	592
$10^4 A_2$ (cm³/g²)	36	16.7	17.2	12.5	3.66
		(b) Debye Analysis[a]			
$10^{-6}M_W$	0.8	0.8	0.7	0.9	0.75
R_G (Å)[b]	965	834	787	677	592

[a] Values for M_W using Debye analysis for the limit $\{Kc/R(\theta=0)\}$ vs c, together with those of the radius of gyration deduced using the molecular weight correction as explained in the text. [b] $R_G = R_G(\text{Zimm}) \times \{M_{\text{Debye}}/M_{\text{Zimm}}\}^{1/2}$.

weight is constant; the value taken is the one provided by Zimm analysis at $c_S = 4.1 \times 10^{-2}$ M. A value $M_W \simeq 8 \times 10^5$ is actually very close to that measured previously using GPC as described in ref 26. It is the first direct and accurate determination of this parameter for the present PPV material. The successful fit of the data to a conventional Zimm plot for high ionic strengths guarantees the reliability of the value hereby reached. The existence of a nonzero third virial coefficient A_3, for the lowest ionic strengths, may be attributed to the emergence of non-negligible three-body interactions, when the screening effects brought by the counterions become weak.

Given the presence of M_W in the slope and intercept of $\{Kc/R(\theta)\}$ (eq 10), a correction for the values of R_G in Table II at each ionic strength deduced from the previous Zimm analysis using the value $M_W = 8 \times 10^5$ [$R_G = R_G(\text{Zimm}) \times (M_{\text{Debye}}/M_{\text{Zimm}})^{1/2}$] provides a better estimate for the polyion size. The corresponding values, listed in Table II, are smaller than the previous case; they will be used in the discussion below. There is no direct effect related to determination of the molecular weight on the estimate of A_2 (see eq 10), even though extrapolation to $q = 0$ may be sensitive to c. However, the last point is present even for neutral systems.[28]

The most important point is the strong dependence of both R_G and A_2 on the ionic strength of the medium. The size of the polyions experiences an increase of about 50% over a reduction of the ionic strength of about 1 order of magnitude: $R_G \simeq 840$ Å for $c_S \simeq 0.56 \times 10^{-2}$ M whereas its value is about 590 Å for $c_S \simeq 4.1 \times 10^{-2}$ M (Figure 4a). Simultaneously, the second virial coefficient A_2 experiences a 1 order of magnitude increase for the same range of counterion concentrations. The important enhancement of R_G and A_2 as c_S is decreased reflects, very well, the competition between the electrostatic repulsive interactions, the screening effects, and their mutual effects on the thermodynamical properties of these solutions.

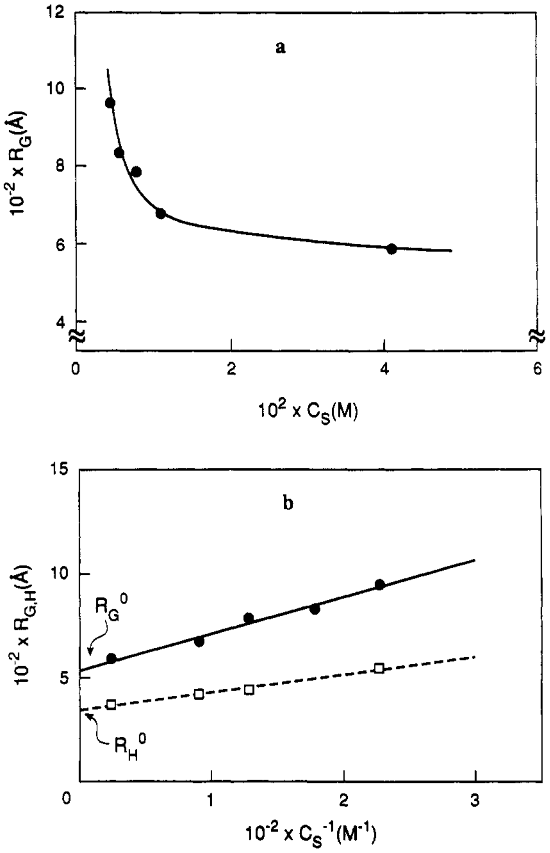

Figure 4. Experimental data for R_G reached using the "Zimm-corrected" analysis (see text): (a) R_G vs c_S; (b) R_G and R_H (from ref 14) vs c_S^{-1}.

Remarks

1. The values for the parameters hereby measured, i.e., R_G, A_2, and M_W, are only "apparent" in principle. They are affected by the refractive index increment. In fact, for a multicomponent system, e.g., polyelectrolyte media, $\partial n/\partial c$ is complex and has contributions from all the components in the solution. An account of this factor has been discussed in ref 28, for instance. These effects may be slightly important only for higher ionic strength in polyelectrolyte solutions, though: $c_S \simeq 0.5$–1 M or larger, for example. Because of the relatively modest salt concentrations scanned in the present case, $c_S < 0.05$ M, the effects on the measured parameters may be neglected. No measurements of the refractive index increment at constant chemical potential $(\partial n/\partial c)_\mu$ were taken. Nevertheless, we checked that the value for $\partial n/\partial c$ at constant c_S was not affected by the ionic strength even when the latter approaches zero. This property together with what has been discussed above (modest ionic strength) would suggest that the value for $\partial n/\partial c$ at given c_S used in the data analysis is not different from the one at constant μ.
2. The emergence of nonlinear terms in the expansion $\{Kc/R(\theta=0)\}$ vs c, for some ionic strengths, does not affect substantially the determination of A_2, if analysis is limited to low-c intervals, as proved in previous work.[28]

3. For polydisperse materials, it is known that, in principle, the plot of $\{Kc/R(\theta)\}$ vs $\sin^2(\theta/2)$ at infinite dilution presents a departure from the linear behavior expected for an ideal monodisperse system in eq 10. A value for $1/M_n$ is reached for the asymptotic limit (large angles); the limit $\theta = c = 0$ provides $1/M_W$, whereas the slope with respect to this limit provides a z average radius of gyration $\langle R_G^2\rangle_z$.[5b] Nevertheless, the absence of a substantial departure from the the linear behavior in the Zimm plot (Figure 1) indicates that the influence of the polydispersity factor on the present measurements is small. Consequently, only the weight-average molecular weight M_W and slightly overestimated values for the radius of gyration $\langle R_G^2\rangle_z$ are measured in the present case. In addition and as mentioned previously, GPC measurements for polyelectrolyte systems are often difficult and not very accurate. Moreover, SALS is not extremely sensitive to modest polydispersity, as explained in ref 5b (Chapter 8, p 444). We will no longer consider the effects related to the polydispersity in the present work.

We now compare the experimental data for R_G and A_2 to other theoretical as well as experimental considerations. The effects of the electrostatic interactions on polyelectrolyte solutions as shown by SALS were observed for other materials.[16,17,28,31] These effects are far from being universal though. A dependence of the type $A_2 \sim (c_S)^{-1/2}$ has been observed for many flexible polyelectrolyte solutions with high charge density.[28] The dependence of R_G on c_S has not attracted the same attention as has that of A_2. Change in the macromolecules expansion caused by ionic strength variation was observed for different materials, however.[28]

In what follows, we present a few arguments based on the nature of the solute chains and the dipoles they carry, the solvent quality, its polarity, the solution ionic strength, and their influence on the range of electrostatic interactions. They will be used, afterward, to provide a description for the experimental data hereby obtained. The same arguments have been introduced previously in order to explain the data for the diffusion coefficients measured for the present system and using QELS study.[14]

On one hand, it has been known that the PPV compound is not soluble in any common, organic or nonorganic solvent.[23-26] Simultaneously, the present compound, PPV precursor, is soluble in only few solvents: methanol and water. The solubility in water is found to be drastically affected by counterion excess. A precipitation process takes place in these solutions for high ionic strengths, for instance.[14,15,25,26] The dissolution of PPV precursor derivatives (with tetrafluoroborate side groups, for instance) was also found to be fairly poor.[26] These properties suggest a rather "bad" solvent quality for the present methanol. The involvement of phenyl rings within the backbone would tend to stretch the chain locally. This will result in a fairly important local stiffness and, consequently, in a high natural persistence length ρ_n. Simultaneously, these two properties, modest solvent quality and locally stretched chain, induce a weak natural contribution to the excluded volume parameter υ_n. Nevertheless, the polyions are still flexible, given the lack of double bonds and the presence of side groups. On the other hand, the modest polarity strength of methanol, together with the relatively weak dipoles carried by the sulfonium side groups, for the PPV precursor, would induce a modest dissociation of the S–Cl bonds. Therefore, the charge density along the polyion backbone could actually be much lower than what is nominally expected if full dissociation of the dipoles took place.

The Debye–Huckel screening parameter κ, introduced above (eq 5), involves another characteristic distance: the Bjerrum length L_B expressed as[3,29-31]

$$L_B = e^2/\epsilon k_B T \tag{14}$$

It is large for small values of ϵ and vice versa. This parameter characterizes the condensation process. A portion of the free counterions in the medium will condense around the polyion backbone, to reduce the effective charge density, if L_B is larger than the nominal distance between neighboring charges (dipoles) along the backbone L_C.[29] This is mostly valid for high dissociation along the solute chains, a process which may take place in the presence of very strong dipoles and high polarity strength of the solvent. A value $L_B \simeq 17$ Å is reached for the present case, which implies that the charge density is at least 3 times smaller than what would be expected if full dissociation of the dipoles along the chain took place ($L_C \simeq 5$ Å is the extreme case). However, given the modest dipoles carried by the chain and the relatively small ϵ for methanol, the electrolyte dissociation along the polyion backbone would be weak, the actual value of L_C may be larger than that of L_B (above), and no condensation should occur in this case. Consequently, a charge density with a separation distance L_B present in these media would be the highest; it is only an "extreme nominal" case.

For the present system, on the one hand, the solute polyion chains are fairly flexible. On the other hand, the screening effects are important given the high ionic strengths to which we have limited our study.[14] Within these conditions, the electrostatic contributions to both persistence length and excluded volume parameters ρ_e and υ_e may have relatively simple expressions written, respectively, as[12-14,30]

$$\rho_e \simeq L_B/4{L_C}^2\kappa^2 \tag{15}$$

and

$$\upsilon_e \sim e^{-\kappa d}/\kappa^2 \tag{16}$$

where d designates the chain cross-section diameter. The electrostatic persistence length ρ_e reduces to a simple expression

$$\rho_e \simeq 1/4L_B\kappa^2 \tag{17}$$

if L_B is larger than L_C; e.g., a condensation process takes place. This expression (eq 17) is only an upper limit for ρ_e since we believe that a weak dissociation is more likely for the present solutions and no condensation process takes place.

For high ionic strengths and for fairly large chain diameter, which is the case, given the chemical structure of the solute polymer chains, the factor κd is large (mostly for the high values of c_S) and the excluded volume contribution υ_e may be neglected. Within the framework of these considerations, one concludes that the electrostatic persistence length ρ_e (eqs 15 and 17) is proportional to the inverse of the salt concentration: $\rho_e \sim 1/c_S$.

For long flexible polyions, in the presence of strong shielding of the repulsions between neighboring charges along the chain, and in the absence of electrostatic contributions to υ, the expression for the radius of gyration may be written as

$${R_G}^2 \simeq {\alpha_n}^2 \frac{L_W \rho_n}{3}\left[1 + \frac{\rho_e}{\rho_n}\right] \tag{18}$$

$\Psi(L_W/\rho)$, in eq 2, is about 1. The expansion factor α_n for the neutral compound may be assumed to be that for the highest ionic strength ($c_S = 4.1 \times 10^{-2}$ M), since $\alpha_e \simeq 0$. However, the second virial coefficient for polyelectrolyte solutions becomes fairly complex because of the electro-

Table III
Values for the Debye Length κ^{-1} and the Electrostatic Persistence Length ρ_e for the Different Ionic Strengths Scanned

$10^2 c_S$ (M)	0.44	0.56	0.78	1.1	4.1
$10^4 \kappa^2$ (Å^{-2})	11.4	14.8	20.70	30.90	106.4
κ^{-1} (Å)	29.6	26	22	18	9.8
ρ_e (Å)	13	10	7	4.75	1.5

static contributions. Many accounts for such contributions have been considered by different authors.[28] The expression introduced above (eq 4) was proved to be also useful for polyelectrolyte solutions (Orifino and Flory).[8b,c,28] Within the framework of the approximations discussed above, $\alpha \simeq \alpha_n$ and $\rho = \rho_n + \rho_e$ as was done for R_G, A_2 may be written as

$$A_2 \simeq \alpha_n^{\ 3}\frac{\pi N_A}{M_W^{\ 2}}\left[\frac{L_W \rho_n}{3}\right]^{3/2} \ln\left\{1 + \frac{\pi^{1/2}}{2}(\alpha^2 - 1)\right\}\left[1 + \frac{\rho_e}{\rho_n}\right]^{3/2} \quad (19)$$

where the constant numbers in eq 4 have been ignored. A dependence of R_G and A_2 on the ionic strength emerges from eqs 5 and 17–19.

Using expressions 5 and 17, for κ^2 and ρ_e, we computed the corresponding values for the Debye–Huckel screening length κ^{-1} and the electrostatic contributions to the persistence length ρ_e; they are listed in Table III. The electrostatic persistence length ρ_e is modest and decreases sharply with increasing ionic strength. Based on the very small value of ρ_e for the highest salt concentration used, we can assume that the corresponding set of solutions is very close to the neutral case. Using the corresponding value for R_G and eq 1 for a wormlike chain, together with the assumption $\alpha_n \simeq 1$ and $\psi(y) \simeq 1$, we reached an estimation for the natural persistence length: $\rho_n \simeq 40$ Å.[14] These assumptions together with neglecting ρ_e compared to ρ provide only an approximate, and overestimated, value for the natural persistence length. Nevertheless, the value hereby reached is large; it is much larger than the value of ρ_e reached at all ionic strengths (see Table III).

The small values for the persistence length ρ_e with respect to the natural term ρ_n, even for the smallest ionic strengths, is consistent with the arguments suggested above, i.e., weak charge density along the backbone and long flexible chains. This condition allows to use the approximation $(\rho_e/\rho_n) \simeq x \ll 1$ in expressions 18 and 19 for R_G and A_2, respectively. Therefore, a linear expansion as a function of the ratio x is a realistic operation for these parameters, and the following expressions result:

$$R_G \simeq R_G^{\ 0}\left(1 + \frac{a}{c_S} + ...\right) \quad (20)$$

$$A_2 \simeq A_2^{\ 0}\left(1 + \frac{b}{c_S} + ...\right) \quad (21)$$

where R_G^0 and A_2^0 designate the corresponding parameters for the asymptotic neutral solutions case ($c_S^{-1} \rightarrow 0$). The constants a and b are expressed as function of ρ_n and L_B:

$$a = \frac{1000}{64\pi N_A \rho_n L_B^{\ 2}} \quad (22)$$

$$b = \frac{3000}{64\pi N_A \rho_n L_B^{\ 2}} \quad (23)$$

Nevertheless, such linear expressions are less accurate for weak screenings (smaller values for c_S). The type of dependence of R_G and A_2 on c_S hereby reached ($\sim 1/c_S$) is compared to the experimental data for the present solutions. Plots of R_G vs $1/c_S$ and for A_2 vs $1/c_S$ are reported in Figures 4b and 5, respectively.

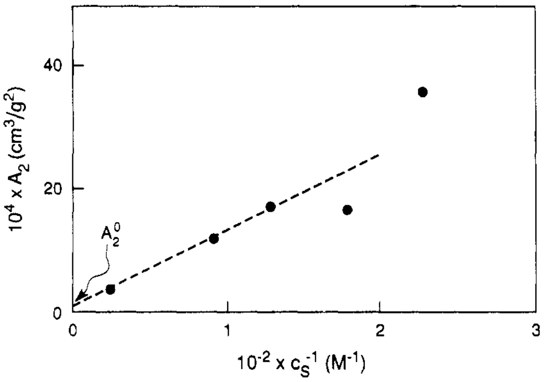

Figure 5. Second virial coefficient A_2 vs inverse ionic strength c_S^{-1}, experimental data from Zimm analysis.

The linear type of dependence reached for R_G vs $1/c_S$ describes well the experimental data for the radius of gyration. The agreement is actually quite good for all ionic strengths scanned. This agreement is not surprising if one keeps in mind that R_G is the extrapolated static size for an isolated chain in the medium. The counterion excess would dominate the Coulomb repulsions within the chain even for relatively small values of c_S, and ρ_e will always be small for infinite dilutions. Eventually, a possible departure from the linear expansion may be observed if much smaller salt concentrations were studied. The same observation has been reached for the hydrodynamic radius R_H as discussed in ref 14. The success of the linear fit for R_G vs $1/c_S$ confirms the validity of the arguments concerning the solvent quality and the modest charge density along the solute chains. Incidentally, we mention that a fit to a different type of power law, $(c_S)^{-1/2}$, for instance, did not provide the same extent of agreement with the experimental data as the one shown in Figure 4b for R_G vs c_S^{-1}. The asymptotic value reached for the radius of gyration at the limit $c_S^{-1} \rightarrow 0$, $R_G^0 \simeq 530$ Å, is reasonable for polymer chains with similar M_W. This value is also very satisfying when compared to the corresponding hydrodynamic radius at the same limit: $R_H^0 \simeq 375$ Å.[14] The ratio $R_G^0/R_H^0 \simeq 1.41$ is in agreement with what has been predicted for polymer solutions ($R_G^0/R_H^0 \simeq 1.5$) in good solvents, and Θ solvents as well.[10] This ratio stays approximately the same over the range of c_S scanned (see Figure 4b). Using eq 22 and the estimation for the persistence length ρ_n, we computed a value for the constant a: $a_{th} \simeq 7 \times 10^{-4}$ (M^{-1}), whereas the corresponding experimental value extracted from the data in Figure 4b is a $a_{exptl} \simeq 3.4 \times 10^{-3}$ (M^{-1}). These values, even though of the same order of magnitude, are still different. This modest success reflects the validity of the "first-order" approximation in evaluating the electrostatic contributions to the radius of gyration. They already provide a good description for the dependence on c_S. Nevertheless, these theoretical considerations could not account, quantitatively, for the electrostatic effects. This may be attributed to an overestimation of ρ_n and also to the picture in which the paramter ρ_e was accounted for; ρ_e given by eq 17 may be overestimated. Neglecting the excluded volume contributions also contributes to this discrepancy.

The fit of the experimental data for the second virial coefficient A_2 to a linear dependence on $1/c_S$ provided a straight line in agreement with eq 21 only for the highest ionic strengths. A departure from the linear dependence is observed for lower salt concentrations (the value of A_2

for $c_S \simeq 0.56 \times 10^{-2}$ M should be considered with some reservations since the corresponding set of solutions provided a slightly smaller value for $\partial_n/\partial c$ than what was measured for the other ionic strengths). This again reflects the success, and the limitations as well, of the present treatment for the electrostatic contributions within the framework of a persistent chain. The linear expansion is successful only for strong screenings as was observed for R_G, R_H, and the diffusion coefficient and where the electrostatic repulsion effects on ρ are small.[14] The departure from the linear behavior for lower ionic strengths may be attributed to the failure of the linear expansion when ρ_e becomes large, and also to an overestimation of ρ_n as mentioned above for R_G. Neglecting the excluded volume would also contribute to this discrepancy. As experimental value for the constant b hereby reached is $b_{\text{exptl}} \simeq 3 \times 10^{-2}$ (M^{-1}). This value is larger than the calculated one using eq 25: $b_{\text{th}} \simeq 2 \times 10^{-3}$ (M^{-1}). The difference between the measured value and expected one may be attributed to an overestimation of both ρ_e and ρ_n, and also to neglecting the excluded volume contributions, as was suggested for the constant a, above. Nevertheless, the success of the linear expansion in describing the scaling of A_2 as c_S^{-1}, in contrast with what has been observed for other flexible polyelectrolytes where a $c_S^{-1/2}$ scaling was reported, confirms the arguments introduced above. The linear variation of A_2 with $c_S^{-1/2}$, observed for polyions with high charge density and in good solvents, is substantially influenced by the contributions to the excluded volume. These effects are fairly complex and require a more extensive study and knowledge of the material.

The present type of behavior, mostly for high ionic strengths, is similar to the Donan picture for charged globular particles. The modest quality of the solvent, the weak charge density along the polyion backbone, and the effectiveness of the shieldings brought by the counterion excess impart a strong reduction of the Coulomb repulsions. This brings the system closer to a solution of "globular" polyions. This qualitative argument is confirmed by the modest value of A_2^0 reached at the limit "$c_S^{-1} \rightarrow 0$": $A_2^0 \simeq 5 \times 10^{-5}$ (cm^3/g^2). In fact, within the framework of expressions 4 and 19 for A_2, the factors introduced earlier and concerning the poor quality of the solvent would translate into a value of α_n close to 1. This would imply a small value for the asymptotic limit A_2^0.

It would be interesting and very helpful to pursue more studies on the present system: measurements of the intrinsic viscosity $[\eta]$, the expansion factor α, and its dependence on the ionic strength, etc. A study of the temperature effects to check if there is any change in the solvent quality may also be useful.

IV. Conclusion

The variation of the macromolecular size R_G and the second virial coefficient A_2 with the ionic strength of the medium has been monitored for flexible polyelectrolyte solutions. Small-angle static light-scattering (SALS) technique has been used to achieve these measurements. The competition between the Coulomb repulsive interactions within the polyions and the screening effects brought by the counterion excess is well reflected in the close dependence of these parameters on the added salt concentration. Both parameters follow a $1/c_S$ type of variation when strong shieldings take place, i.e., for high ionic strengths. This was accounted for within the framework of a flexible wormlike chain with electrostatic contributions to the persistence length. The linearization of the expressions for R_G and A_2 as function of the electrostatic persistence length was appropriate because of the modest contributions of the electrostatic interactions. This is favored by the modest quality of the solutions and is valid mainly for high salt concentrations. A more complex treatment, eventually accounting for the excluded volume contributions, is required if a more rigorous comparison with theory and dependencies at low ionic strength are to be considered.

Acknowledgment. We thank Lark Inc. who provided us with the compound we used. We benefitted from fruitful discussions and suggestions from G. C. Berry (Carnegie Mellon University), J. F. Joanny (CRM Strasbourg), and K. H. Langley (University of Massachusetts). This work was supported by AFOSR Grant No. 88-001.

References and Notes

(1) Flory, P. J. *Principles of Polymer Chemistry*; Cornell University Press: Ithaca, NY, 1953.

(2) Tanford, C. *Physical Chemistry of Macromolecules*; Wiley: New York, 1961.

(3) Yamakawa, Y. *Modern Theory of Polymer Solutions*; Harper and Row: New York, 1971.

(4) Cassassa, E. F.; Berry, G. C. In *Comprehensive of Polymer Science*; Allen, S. G., Bevington, J. C., Booth, C., Price, C., Eds.; Pergamon Press: Oxford, 1989; Vol. 2, Chapter 2.

(5) (a) *Electromagnetic Scattering*; Kerker, M., Ed.; McMillan Publishing: New York, 1963. (b) Kerker, M. *The Scattering of light and other electromagnetic radiation*; Academic Press: New York, 1969. (c) *Small Angle Scattering*; Glatter, O., Kratky, O., Eds.; Academic Press: London, 1982. (d) Mattoussi, H.; Ober, R. *Macromolecules* **1990**, *23*, 1809.

(6) Kuhn, W. *Kolloid Z.* **1936**, *76*, 258; **1939**, *87*, 3.

(7) Benoit, H.; Doty, P. *J. Phys. Chem.* **1953**, *57*, 958.

(8) (a) Flory, P. J.; Bueche, A. M. *J. Polym. Sci.* **1958**, *27*, 219. (b) Orifino, T. A.; Flory, P. J. *J. Chem. Phys.* **1957**, *26*, 1067. (c) Orifino, T. A.; Flory, P. J. *J. Phys. Chem.* **1959**, *63*, 283.

(9) Morawetz, M. *High Polymers*; Wiley: New York, 1975.

(10) Berry, G. C. In *Encyclopedia of Polymer Science & Engineering*; Mark, H., Overberger, C. G., Eds.; Wiley: New York, 1987; Vol. 8, p 721.

(11) Odijk, T. *J. Polym. Sci., Polym. Phys. Ed.* **1976**, *15*, 477.

(12) Odijk, T.; Howart, A. C. *J. Polym. Sci., Polym. Phys. Ed.* **1977**, *16*, 627.

(13) Skolnick, J.; Fixman, M. *Macromolecules* **1977**, *10*, 944.

(14) (a) Mattoussi, H.; Karasz, F. E.; Langley, K. H. *J. Chem. Phys.* **1990**, *93*, 3593. (b) Mattoussi, H.; Langley, K. H.; Karasz, F. E. In *Macromolecular Liquids*; Materials Research Society Symposium; Safynia, C. R., Safran, S. A., Pincus, P. A., Eds.; MRS: Pittsburgh, 1990; Vol. 177, p 71.

(15) Mattoussi, H. *J. Phys. (Paris)* **1990**, *51*, 2321.

(16) Lin, S. G.; Lee, W. L.; Schurr, J. M. *Biopolymers* **1978**, *17*, 1041.

(17) Schurr, J. M. *Chem. Phys.* **1980**, *45*, 119.

(18) de Gennes, P. G.; Pincus, P. A.; Velasco, R. H.; Brochard, F. *J. Phys. (Paris)* **1976**, *37*, 1461.

(19) Debye, P. *J. Phys. Coll. Chem.* **1947**, *51*, 8.

(20) Zimm, B. H. *J. Chem. Phys.* **1948**, *16*, 1093.

(21) Kratochvil, P. In *Light Scattering from Polymer Solutions*; Huglin, M. B., Ed.; Wiley: New York, 1972, Chapter 7.

(22) Reference 2, Chapter 5.

(23) Machado, J. M. Ph.D. Dissertation, Polymer Science and Engineering Department, University of Massachusetts, 1988.

(24) Gagnaon, D. R.; Capistran, J. D.; Karasz, F. E.; Lenz, R. W. *Polym. Bull.* **1984**, *12*, 293.

(25) Gagnaon, D. R.; Capistran, J. D.; Karasz, F. E.; Lenz, R. W.; Antoun, S. *Polymer* **1987**, *28*, 567.

(26) Machado, J. M.; Denton, F. R., III; Schlenoff, J. B.; Karasz, F. E.; Lahti, P. *J. Polym. Sci., Polym. Phys. Ed.* **1989**, *27*, 199.

(27) Swiatkiewicz, J.; Prasad, P. N.; Karasz, F. E.; Druy, M.; Glatoski, P. *Appl. Phys. Lett.* **1990**, *56*, 892.

(28) Nagasawa, M.; Takahashi, A. In *Light Scattering from Polymer Solutions*; Huglin, M. B., Ed.; Wiley, New York, 1972; Chapter 16, and references therein.

(29) Manning, G. *J. Chem. Phys.* **1969**, *51*, 924.

(30) Berry, G. C. In *The Materials Science & Engineering of Rigid Rod Polymers*; MRS Symposium; Adams, W. W., Eby, R. K., Lemore, D. E., Eds.; MRS: Pittsburgh, 1989; Vol. 134, p 181.

(31) Nicolai, T.; Mandel, M. *Macromolecules* **1989**, *22*, 438.

Registry No. Poly(*p*-xylylene tetrahydrothiophenium chloride), 115708-89-9.